A search for R-parity violating Supersymmetric top decays at CMS with $\sqrt{s} = 8$ TeV

Alec Aivazis[1] and Ari Kaplan[1]

[1]Affiliation not available

September 27, 2021

1 Introduction

With the discovery of the Higgs, the Standard Model seems to offer a complete tally of the fundamental particles with which all of the matter around us is made.(Aad and et al, 2012) However, with this answer comes more questions as phenomena such as the origin of dark matter and the seemingly unnatural Higgs mass remain unanswered, and cause theorists to look for physics beyond the Standard Model.

Supersymmetry is one such theory and proposes an extension to space-time which allows for a symmetry relating the two groups of fundamental particles: fermions and bosons, where each of the particles from one group have a corresponding supersymmetric partner differing by half-integer spin. These supersymmetric partners provide opposite quantum corrections to the mass of the Higss and thus yield a natural explanation for the Higss mass. Associated with this extension is a quantum number R, defined as

$$R = (-1)^{(3B+L+2S)} \tag{1}$$

where S, B, and L, are the spin, baryon, and lepton quantum numbers of the particle.(Huh et al., 2009)

It is important to note that due to the definition of this quantum number, particles in this theory must be created in a pair-wise fashion. Because of this, this quantum number is refered to as 'R-parity.' It is also important to note that Supersymmetric particles have an R value of -1 whereas particles that are of the Standard Model have R = 1.

In order for energy and R-parity to be conserved, Supersymmetric particles must decay pair-wise through a series of intermediate processes and have an eventual final state of lighter Standard particles and some number of the lightest supersymmetric particle (LSP).(Berger et al., 2013) However, if R-parity is not conserved, a Supersymmetric particle can have a final state which consists only of particles found in the Standard Model.

While there have been a few searches for R-parity violating decays in the past, R-parity conserving theories are more widely researched as they provide an explanation for the massive prevalence of seemingly weakly interacting dark matter.(Trotta et al., 2007)(Lahanas, 2007) However, there is little reason to believe *a priori* that spacetime would behave in such a way as to conserve R_p. Coupling this with the increased capacity for data collection available to the Compact Muon Solenoid (CMS) at LHC at CERN, it is necessary to perform searches for these decays using new techniques which might uncover possibly interesting results.

This paper describes a search for such a decay of the form:

$$\widetilde{t}\widetilde{t}^{*} \to \mu^{+}\mu^{-} b\bar{b} \tag{2}$$

Since the signature of this decay resembles that of many common Standard Model vertices, various data-based background estimation techniques were implemented in conjunction with Monte Carlo simulations to obtain a number of expected events. For a detailed description of these techniques see section 3.

2 The CMS detector

FIX ORDER The primary feature of the CMS detector is a superconducting solenoid that is 6m in diameter, 13m long, and generates a 3.8T field which is used to determine the sign of the charge of the particle, as well as it's momentum. On the inside of the magnet is an electromagnetic calorimeter (ECAL) which is made of lead tungstate crystals and collects and measures electromagnetic deposits. This primarily detects electrons and photons, muons are more massive and therefore have more energy to deposit before being stopped, allowing them to travel past the ECAL and further into the detector. The ECAL surrounds a silicon tracker which matches particle interactions with other areas of the detector in order to reconstruct trajectories. Inside the tracker is the beam pipe in which particles are accelerated by the superconducting solenoid. After the products of the decay have passed through the tracker and ECAL they reach a hadronic calorimeter (HCAL) made of dense brass and steel designed to stop the massive energy deposit from hadronization, this absorbs most of the energy left in the collision. The particles that do make it through the HCAL are either neutrinos or muons. The muons are detected and collected in a separate configuration around the magnet composed of a drift tube and cathode-strip detector and since the effects of baryonic matter on neutrinos is taken to be negligible by the cross section, neutrinos appear in the data as missing energy in the transverse direction (MET).(AUFFRAY, 2002)(Pooth, 2010)(Khachatryan and et al, 2014)

CMS uses a right-handed coordinate system whose origin is at the point of interaction between the two proton beams, x-axis pointing to the center of the LHC, y-axis perpendicular to the plane created by the beam, and z-axis in the anticlockwise-beam direction. θ measured from the positive z-axis.(Khachatryan and et al, 2014) For a detailed description of the CMS detector see (Collaboration and et al, 2008).

3 Event selection and Monte Carlo simulation

Each event is processed using a global event reconstruction algorithm which reconstructs and indentifies the particles using information from all of the subdetectors as described in section 2. It is important to note that this algorithm relies heavily on the identifacation of the particle type (photon, electron, muon, hadron) to reconstruct the trajectory of the particle.(Khachatryan and et al, 2014) After events are reconstructed, they are selected from an online dilepton trigger (events only include those whose final state constain ee, $e\mu$, μe, and $\mu\mu$) which requires the tranverse momentum (p_T) of the largest lepton to be greater than 17 GeV and the smaller to be greater than 8 GeV.

The reconstructed trajectories (known as hypotheses) are then grouped together according to the location in the LHC where the interaction occured. This is done to prevent particles that originated in other interactions (pileup) from being considered as part of the final state. Each hypothesis is restricted to non ee events with $p_T > 20$ GeV, oppositely charged leptons, $|\eta| < 2.4$ where $\eta \equiv -\ln\frac{\theta}{2}$, and have a total invariant mass greater than 20 GeV. A minimum isolation is also required according to the loose working points of the combined secondary vertex (CSV-L) algorithm. (Khachatryan and et al, 2014) The hypothesis with the highest combined p_T bewtween the two leptons that passes these criteria is then taken to be the primary interaction at the corresponding LHC bunch crossing.

After the primary hypothesis has been found, the hadronic jets corresponding to the event are reconstructed using the anti-k_T algorithm.(Cacciari et al., 2008) The jet momentum is determined as the vector sum of all particle momenta in the jet. For this analysis, the jets considered are required to be inside the tracker acceptance ($|\eta| < 2.4$) as well as a scaled $p_T > 20$ GeV. The primary jets are taken to be the two jets in the bundle which when paired with the leptons in the primary hypothesis, minimize the total invariant mass.

This is done under the assumption that the most likely process to occur is the one with the smallest amount of p_T. Once the event jets have been reconstructed, the collection of primary hypotheses are then restricted to those events with a $p_T > 20$ GeV as well as requiring at least 2 jets to have passed the criteria above. A minimum combined invariant mass of 20 GeV as well as a minimum difference in mass between the two pairings of 100 GeV is set to prevent events containing fakes and photons to be considered in the analysis. In order to prevent events originating from a process similar to Drell-Yan, a z-veto was added to the selection criteria by restricting events to having a combined invariant momentum that does not fall within 15 GeV of the mass of the Z-boson (approx 91 GeV).

For analysis in which the mass of the supersymmetric top was less than 700 GeV, the events were required to have an average invariant mass of the lepton/jet pair within 50 GeV of the stop mass, missing transverse energy (met) ≤ 60 GeV and at least 1 b-tagged jets. For analyses where m_{stop} is at least 700 GeV, the b-tag requirement was increased to at least 2 such jets.

For computations that try to encapsulate the behavior of the algorithms (see sect 4 for more information) two separate control regions were considered. The dy dominated control region required to have an average mass of the lepton/jet pair < 250, met ≥ 60 and at least 2 of the jets reconstructed must be b-tagged according to the CSV-L algorithm. By requiring two b-tagged jets the control region is restricted to those final states which closely resemble our target decay. And the tt dominated region required the same cuts with an inverted met requirement.

Monte Carlo simulations of initial state samples for the target process were generated in Pythia 6 assuming a mass for the supesymmetric top at 50 GeV intervals between 200 and 800 GeV. These samples were then decayed to their final state using MadGraph5 v1.5.11.(Płaczek et al., 2013)(Alwall et al., 2011) For a description of the various background estimations, see sections 4 and 5.

4 Background estimation

There are 2 processes that contribute the most to the background signal. The first is a Drell-Yan decay of the form

$$Z \to \mu^+\mu^- b\bar{b} \tag{3}$$

and will later be referred to as dy.

The second biggest background (to be reffered to as $t\bar{t}$) is a two step decay in which a t and a $\bar{t}$ both decay to the corresponding b-quark and a W-boson which subsequently decays to a muon and its neutrino :

$$t\bar{t} \to W^+W^- b\bar{b} \to \mu^+\mu^- b\bar{b}\nu\bar{\nu}* \tag{4}$$

While these two contribute the most to the background signal, there are 6 other proceses which have signatures that can resemble the target decay after taking into consideration fakes and mismeasurements. Those processes are:

$$\begin{aligned} WZ &\to 2\ell 2q* \\ &\to 3\ell\nu* \\ WW &\to 2\ell 2\nu* \\ ZZ &\to 4\ell \\ &\to 2\ell 2\nu \\ &\to 2\ell 2q \end{aligned} \tag{5}$$

Of these 8 backgrounds, the processes with a * after them exhibit a 2-to-1 ratio of $e\mu$ to $\mu\mu$ events as the final state. Using this, the number of $\mu\mu$ events present in the data that come from these background processes can be estimated from the total number of $e\mu$ events present in data. However, due to experimental variations, we do not expect $\frac{N_{e\mu}}{N_{\mu\mu}} = 2$. For this reason, the actual number used is computed in the tt dominated control region using the ratio of $e\mu$ events to $\mu\mu$ events in data, subtracting off the events from non 2:1 backgrounds. This ratio was found to be $R_{2:1} = 2.01 \pm 0.033$

For those processes which do not exhibit the 2-to-1 ratio, the expected number of events is computed based on estimates produced by the Monte Carlo samples discussed in section 3. Since the Monte Carlo simulations cannot be assumed to be perfect, the estimates for the non 2-to-1 processes were scaled based on the ratio in the dy dominated control region of non 2-to-1 processes in data to those in Monte Carlo, i.e. $SF = \frac{N_{data} - N_{2:1}}{N_{non-2:1}}$. Where N corresponds to the number of $\mu\mu$ events in the dy dominated control region.

While these numbers, calculated for each mass point, varied slightly, a χ^2 test (Adke, 1994) resulted in a 47% confidence that they varied around the mean value in the 200-450 GeV region and a 96% confidence in the 500 GeV and above region. While the confidence level for the first region appears to be low, large variances in these uncertainties have very minor effects and these minutia can be considered negligible. Therefore a weighted average of the calculated values in the 200-450 GeV region and the greater than 500 GeV region were used in making our final prediction.

The final expression for the total count is as follows

$$\text{Total Pred} = (\mathrm{D}_{\mathrm{e}\mu} \div R_{2:1}) + (SF \times \mathrm{N}_{\mathrm{non}-2:1}) \tag{6}$$

where $R_{2:1}$ and SF are defined as above, $D_{e\mu}$ refers to the number of $e\mu$ events in data, and $N_{non-2:1}$ refers to the number of non 2-to-1 $\mu\mu$ events in Monte Carlo.

5 Systematic uncertainties in signal region

Gaussian statictics were assumed for calculating statistical uncertainties. The baseline systematic uncertainties were adapted from (Khachatryan and et al, 2014) as it has focuses on a similar kinematic region. This included a 2.6% uncertainty to account for mismeasurement of the luminosity, a 6% uncertainty added for each lepton in the requirement, a 4% uncertainity was added due to trigger efficiencies, and finally an additional 2% for each b-tagged jet required as part of the signal region.

In order to deduce a systematic uncertainty associated with the scaling of the jet energy, the factor used to scale was increased and decreased by a fixed amount. The two relative differences from the original value were averaged together to produce a single number for a given mass point. This process resulted in a systematic uncertainty of 2% to be added to the analysese where the supersymmetric top's mass was below 500 GeV. A 3% uncertainty was added to those events where m_{stop} falls between 550 and 700 GeV and a 4% uncertainty was added to the analysis at higher mass points.

Uncertainties associated with the dy based scale factor were found by finding the difference in the scale factor between the signal region and the dy dominated control region. This difference was then averaged over to produce a final systematic error due to S_{dy}. For those events where m_{stop} falls between 200 and 450 Gev, this uncertainty was 10%. For analyses with higher mass points, this uncertainty increased to 25%.

6 Results

Since the mass of the decaying super symmetric top is unknown, many such analyses were performed assuming a different m_{stop} in order calculate a potential regime in which the data allows for a decay of the signature

m_{stop}	Total Pred	Data
200	667.9 ± 46	735
250	262.8 ± 26.4	255
300	83.2 ± 12.5	94
350	35.5 ± 8.1	41
400	18.4 ± 6.4	14
450	2.1 ± 4.7	2
500	3.3 ± 3.7	4
550	2.8 ± 3.8	4
600	4.1 ± 3.8	1
650	0.52 ± 3.6	0
700	.04 ± 3.1	0
750	0.01 ± 3.1	0
800	0 ± 3.1	0

Table 1: The final count for events passing the criteria discussed in section 3. For the upper limits set on the cross section of these processes see section 6. For a plot of these values as well as a comparison of contributions from the various backgrounds, see figure 4.

discussed in section 1. For a summary of the total number of events predicted that match the signature for a particular m_{stop} see table 1 and a visualization of this data can be seen in figure 4.

Apart from raw event count, a plot of the average mass vs the difference in mass between the lepton/jet pair for each event provides a nice picture of the various final states present in the sample. The spread in ΔM provides an graphical representation for the amount by which the two particles came from the same parent and the spread in $< M >$ provides an understanding for the mass of the parent particle. As you can see in figure 1, the data (left) shows that most events came from Z-bosons like the *dy* process discussed in 4 as evident by the large collection of points centered around 90-100 GeV. Comparing this to a few of the same plots with only signal Monte Carlo (right), the data plot does not seem to contain a substaintial number of events that match our signature in any of the mass regions.

Table 1 illustrates the existance of an m_{stop} for which the data could contain enough events that match the target signature to count as evidence for the target decay. In order to investigate this, an upper limit on the cross section was calculated based on the number of events in each signal region. This plot was overlayed with the cross section used during signal simulation and a cut-off point is extracted. See fig 2 for more information. From this, a lower limit on the mass of the supersymmetric top is set to 780 GeV.

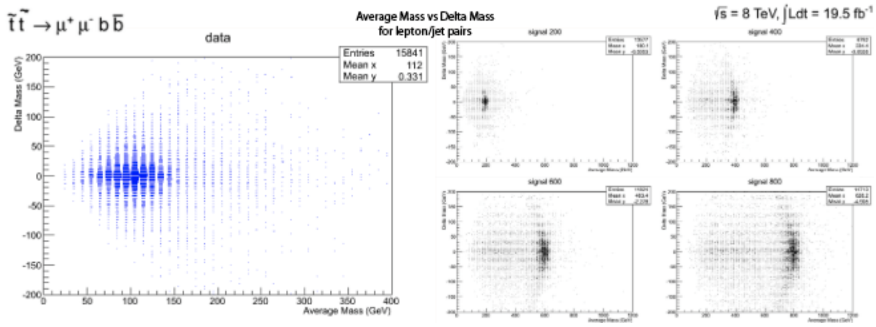

Figure 1: The difference in mass bwetween lepton/jet pair in fata (left) and various Monte Carlo samples of the target decay as discussed in section 1. The spread in ΔM provides an graphical representation for the amount by which the two particles came from the same parent and the spread in the average M provides an understanding for the mass of the parent particle. As you can see in figure 1, the data (left) shows that most events came from Z-bosons like the *dy* process discussed in 4 as evident by the large collection of points centered around 90-110 GeV. From this, it is clear that the data is unlikely to contain the target decay as there does not seem to be any bunches of events that would indicate it as shown on the left graphs.

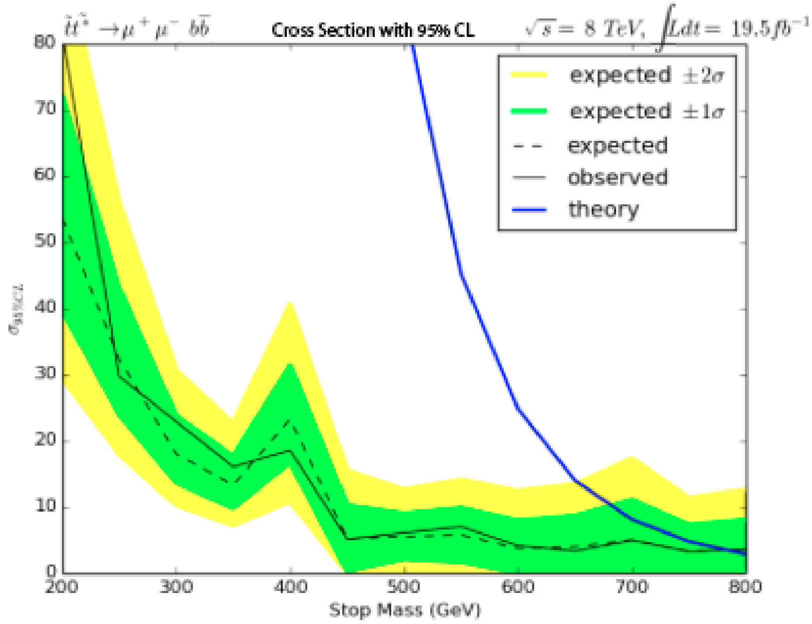

Figure 2: Using Baysian marginalization, an upper limit on the cross section is computed to a 95% confidence level. For a summary of the event numbers that produced these results see table 1. This plot shows that below 750 GeV, the calculated cross section is lower than expected, resulting in fewer events that match the target signature. Above 780 GeV, however, the calculated upper limit on the cross section is higher than expected resulting in more events in data than what we expected.

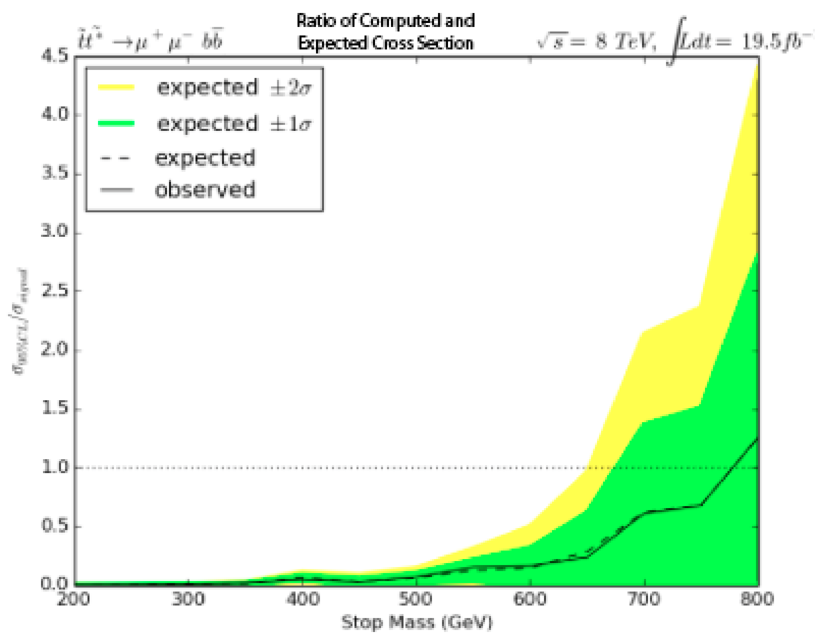

Figure 3: The ratio of the calculated cross section to the expected value assuming a minimally supersymmetric model. Where the line crosses 1 determines the cut off point for the regime in which the data cannot support the existence of enough events with the matching signature to say it is present. Past the 780 GeV mass point, there are more events in data with the target signature than expected by theory. Therefore, there is not enough data to determine whether or not there is an event that matches the target decay as discussed in section 1.

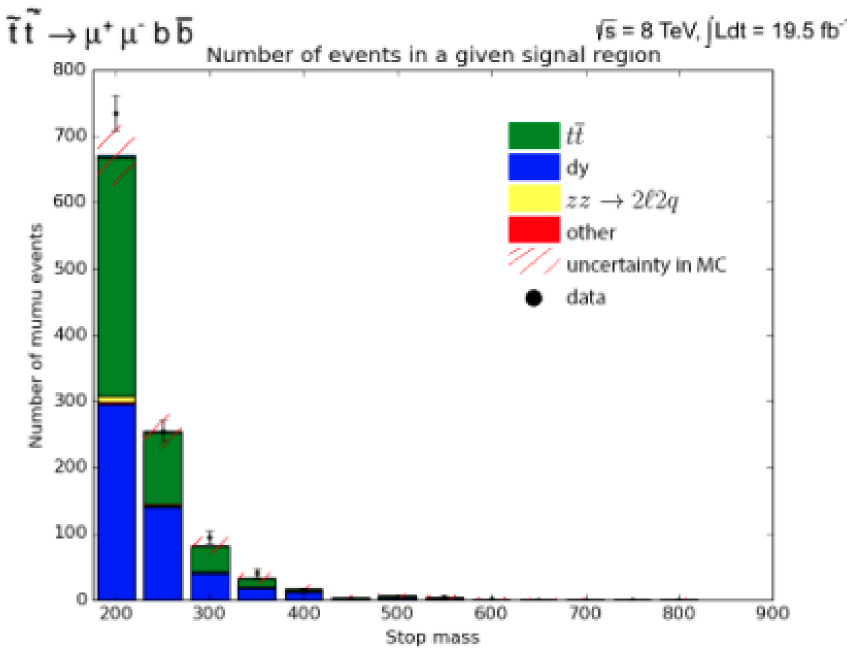

Figure 4: This graph shows a comparison between the number of events that passed the selection criteria discussed in section 3 that were present in data (black dot) versus the total number of events present in all of the background Monte Carlo simulations. From this, it's clear that while statistical uncertainties seem be high enough to consider them matching, the Monte Carlo's do not do as good of a simulating the detector's behavior at lower mass points as they do at higher energies. This can be attributed to the accuracy with which we model QCD at low energies.

7 Summary and Discussion

A search for a supersymmetric top which decays with 100% probability in the follow way

$$\widetilde{t}\widetilde{t}^* \to \mu^+\mu^- b\bar{b} \tag{7}$$

was presented using the CMS detector at an integrated luminosity of 8 TeV. While the presence of the signal cannot be determined conclusively from the data, a limit was calculated based on the event yields and it was found that this signature cannot be present in the data set if $m_{\text{stop}} < 780$ GeV. For a summary of the event yields see section 6. For a plot of the upper limits calculated from the event yields see figure 2.

Comparing this minimum weight to the particles of the Standard Model, it would appear that the liklihood the supersymmetric top has an invariant mass > 780 GeV is low. Thus these results provide more compelling reasons for theorists to look for other possible decays modes for the supersymmetric top which might contribute to a higher cross section. Also, these results show that given more data, we should be able to expect enough statistics to calculate a larger minimum value, pushing the possiblity of a decay mode of this branching ratio being supported by the data closer to zero. Therefore, it would be useful to perform this analysis again once the Large Hadron Collider reaches its maximum capacity in the coming years.(Moskowitz, 2014)

8 Acknowledgements

We would like to thank the technical and administrative staffs at CERN and other CMS institutes for their contributions to the success of the CMS experiment. In addition, we would like to acknowledge the efforts put forth by the computing centers and personnel of the Worldwide LHC Computing Grid for maintaining the computer infrastructure necessary for this analysis. We would also like to thank those supporting the construction and operation of the LHC and the CMS detector. Special thanks also to the DOE for its source of funding, the Worster Family for their support of our summer research, as well as other worldwide funding organizations who have contributed to CMS.

In addition to personnel at CERN, we would like to thank Claudio Campagnari, Frank Golf, Alex George, and Jason Gran at the University of California, Santa Barbara for their continued help during this analysis.

References

G. Aad and et al. Observation of a new particle in the search for the Standard Model Higgs boson with the ATLAS detector at the LHC. *Physics Letters B*, 716(1):1–29, sep 2012. doi: 10.1016/j.physletb.2012.08.020. URL http://dx.doi.org/10.1016/j.physletb.2012.08.020.

S.R. Adke. Optimum statistical inference from randomly stopped random processes. *Journal of Statistical Planning and Inference*, 39(2):255–271, apr 1994. doi: 10.1016/0378-3758(94)90208-9. URL http://dx.doi.org/10.1016/0378-3758(94)90208-9.

Johan Alwall, Michel Herquet, Fabio Maltoni, Olivier Mattelaer, and Tim Stelzer. MadGraph 5: going beyond. *Journal of High Energy Physics*, 2011(6), jun 2011. doi: 10.1007/jhep06(2011)128. URL http://dx.doi.org/10.1007/JHEP06(2011)128.

E. AUFFRAY. CMS/ECAL BARREL CONSTRUCTION AND QUALITY CONTROL. In *Calorimetry in Particle Physics - Proceedings of the Tenth International Conference*. World Scientific Publishing Co. Pte. Ltd., 2002. doi: 10.1142/9789812704894_0026. URL http://dx.doi.org/10.1142/9789812704894_0026.

Joshua Berger, Maxim Perelstein, Michael Saelim, and Philip Tanedo. The same-sign dilepton signature of RPV/MFV SUSY. *Journal of High Energy Physics*, 2013(4), apr 2013. doi: 10.1007/jhep04(2013)077. URL http://dx.doi.org/10.1007/JHEP04(2013)077.

Matteo Cacciari, Gavin P Salam, and Gregory Soyez. The anti- k t jet clustering algorithm. *J. High Energy Phys.*, 2008(04):063–063, apr 2008. doi: 10.1088/1126-6708/2008/04/063. URL http://dx.doi.org/10.1088/1126-6708/2008/04/063.

The CMS Collaboration and et al. The CMS experiment at the CERN LHC. *J. Inst.*, 3(08):S08004–S08004, aug 2008. doi: 10.1088/1748-0221/3/08/s08004. URL http://dx.doi.org/10.1088/1748-0221/3/08/S08004.

Ji-Haeng Huh, Jihn Kim, and Bumseok Kyae. Two dark matter components in dark matter extension of the minimal supersymmetric standard model and the high energy positron spectrum in PAMELA/HEAT data. *Physical Review D*, 79(6), mar 2009. doi: 10.1103/physrevd.79.063529. URL http://dx.doi.org/10.1103/PhysRevD.79.063529.

V. Khachatryan and et al. Measurement of top quark–antiquark pair production in association with a W or Z boson in pp collisions at $$\sqrt{s} = 8$$$ s = 8 $$\,\text {TeV}$$ TeV. *The European Physical Journal C*, 74(9), sep 2014. doi: 10.1140/epjc/s10052-014-3060-7. URL http://dx.doi.org/10.1140/epjc/s10052-014-3060-7.

Athanasios Lahanas. LSP as a Candidate for Dark Matter. In *The Invisible Universe: Dark Matter and Dark Energy*, pages 35–68. Springer Science + Business Media, 2007. doi: 10.1007/978-3-540-71013-4_2. URL http://dx.doi.org/10.1007/978-3-540-71013-4_2.

Clara Moskowitz. LHC upgrades could reveal whether Higgs boson is 'standard'. *Nature*, jun 2014. doi: 10.1038/nature.2014.15478. URL http://dx.doi.org/10.1038/nature.2014.15478.

W. Płaczek, S. Jadach, and M.W. Krasny. Drell–Yan Processes with WINHAC. *Acta Phys. Pol. B*, 44(11): 2171, 2013. doi: 10.5506/aphyspolb.44.2171. URL http://dx.doi.org/10.5506/APhysPolB.44.2171.

Oliver Pooth. The CMS Silicon Strip Tracker. In *The CMS Silicon Strip Tracker*, pages 39–86. Vieweg+Teubner, 2010. doi: 10.1007/978-3-8348-9639-1_3. URL http://dx.doi.org/10.1007/978-3-8348-9639-1_3.

Roberto Trotta, Roberto Ruiz de Austri, and Leszek Roszkowski. Direct dark matter detection around the corner? Prospects in the Constrained MSSM. *J. Phys.: Conf. Ser.*, 60:259–263, mar 2007. doi: 10.1088/1742-6596/60/1/056. URL http://dx.doi.org/10.1088/1742-6596/60/1/056.